Journal of Materials and Environmental Sciences
ISSN : 2028-2508

JMES, 2017 Volume 8, Issue 8, Page 2993-3012

http://www.jmaterenvironsci.com/

Removal of Acid Orange 7 Dye from Aqueous Solution Using the Exchange Resin Amberlite FPA-98 as an Efficient Adsorbent: Kinetics, Isotherms, and Thermodynamics Study

S. Akazdam[1*], M. Chafi[1], W. Yassine[1], B. Gourich[1]

1. *Laboratory of Engineering, Processes and Environment (LEPE) , High School of Technology University Hassan II Casablanca Morocco.*

Received 20 Jun 2016,
Revised 17 Oct 2016,
Accepted 23 Oct 2016

Keywords

- ✓ Wastewater,
- ✓ Adosorption,
- ✓ Acide orange 7,
- ✓ Removal,
- ✓ Amberlite,
- ✓ Dyes;
- ✓ Kinetics;
- ✓ Equilibrium;
- ✓ Thermodynamics.

S. Akazdam
said.akazdam@gmail.com
+212658103434

Abstract

In this study, the removal of Acid Orange 7 dye from wastewater using the macroporous strongly basic anion exchange resin Amberlite FPA-98 was investigated using the batch method. The adsorbent was characterized by Fourier Transform-Infrared Spectroscopy (FTIR) and X Ray Diffraction (XRD). FTIR results showed complexation and ion exchange appear to be the principle mechanism for AO7 adsorption. Batch adsorption studies were carried out under various parameters such as contact time, pH, initial dye concentration, adsorbent dosage, agitation speed, and solution temperature on the removal of AO7. Experimental isotherm data were analyzed using Langmuir, Freundlich and Temkin isotherm equations and the isotherm constants were calculated using linear regression analysis for the determination of the isotherm parameters which describe the adsorption process. The best fit was obtained by Langmuir model with a Langmuir maximum monolayer adsorption capacity of 200 mg/g at 303°K. A comparison of kinetic models applied to the adsorption of AO7 onto Amberlite FPA-98 was evaluated for the pseudo-first-order, the pseudo-second-order, Elovich, intraparticle diffusion and Bangham's kinetics models. The adsorption kinetic data were properly fitted very well with the pseudo-second-order kinetic model. The results obtained show that the concentrated solution gives better removal efficiencies. The thermodynamic parameters were evaluated. The negative values of $\Delta H°$ =-118,34 kJ/mol and $\Delta S°$ = -396.8272 J/K.mol indicated respectively that the adsorption of AO7 onto Amberlite FPA-98 was exothermic, spontaneous process. The Gibbs energy ($\Delta G°$) increased when the temperature was increased from 298 to 323°K indicating a decrease in feasibility of adsorption at higher temperatures. The results have established good potentiality for the Amberlite FPA-98 to be used as a sorbent for the removal of AO7 from wastewater.

1. Introduction

Textile industry is very greedy in water and thus, [1] generates an important quantity of effluents highly charged with pollutants which constitute a serious threat for the environment. Consequently, these effluents require a preliminary treatment in order to decrease their polluting load before being rejected into the natural environment. It is considered that the textile industry is responsible for 15% to 20% of the global water pollution [2]. Among the discharged pollutants, organic dyes that are not only responsible for an esthetic pollution of water, but also count among the most toxic compounds, even at low concentration [3]. Today, about 10,000 different dyes are produced worldwide, for a global production of 7.105 tons per year [4]. Dye effluents discharged from the dyestuff manufacturing, dyeing, printing and textile industries represent a serious problem all over the world. They contain

different types of synthetic dyes which are known to be a major source of environmental pollution in terms of both the volume of dye discharged and the effluent composition [5]. Most of these dyes are toxic, mutagenic and carcinogenic [6]. From an environmental point of view, the removal of synthetic dyes is of great concern. The annual worldwide production of dyes is approximated at 800,000 tonnes and about 50% of these are azo dyes [7]. Anionic azo dyes contain many compounds from the most varied classes of dyes . A long known, inexpensive, but only moderately fast dye is C.I Acid Orange 7 (Orange II). As a wool dye it is now of secondary importance, however, it is used in special areas such as leather dyeing and paper coloration. Like most other azo dyes, it tends to be disposed in industrial wastewater and poses a severe health threat to humans. It is highly toxic, and its ingestion can cause eye, skin, mucous membrane, and upper respiratory tract irritation; severe headaches; nausea; water-borne diseases.
In general, chemical and physical discoloration methods have been used for dye removal from wastewaters [8] such as coagulation and flocculation processes which are largely used for wastewater treatment in the textile industries. However application of these methods is somewhat restricted due to some limitations such as operational costs, formation of hazardous by-products, intensive energy requirement and limited adaptability to a wide range of effluents and these processes are not always effective for dye removal. Moreover, they can sometimes generate secondary pollution due to the excessive use of chemical reagents. However, the adsorption of this dye on efficient solid supports is considered as a simple and economical method for its removal from water and wastewater providing sludge-free cleaning operations and many studies have been conducted to find suitable adsorbents to reduce Acid Orange 7 concentration [9]. If a physico-chemical treatment based on adsorption using activated carbon is a possible alternative, this process remains expensive because of the cost of this adsorbent and the difficulty of its regeneration. As a result, the applicability of adsorption process strongly needs low cost natural adsorbents, which are also effective. Among these they have included spent brewery grains [10], guava seed carbon [11], de-oiled soya [12], bottom ash [13], sludge [14], activated carbon fibers [15] chitosan [16] starch [17] bentonites [18], titania aerogels [19], titaniumdioxide [20] zeolites [21], soil [22], and Sahara desert sand [23] clays.
A number of exchange resins have been used quite efficiently for the removal of specific organic compounds [24], this study investigates the adsorption characteristics of Acid Orange 7 dye on the strongly basic polyacrylic anion exchanger Amberlite FPA-98 of macroporous structure. The present work deals with the estimation of the adsorption properties of Amberlite FPA-98 that constitutes a possible source of adsorbent that could be used for the removal of dyes from textile wastewater and, more generally, in industrial wastewater .

The focus of the present study was to assess the potentiality of Amberlite FPA-98 as an adsorbent for the dye AO7 from aqueous solution as an ideal alternative to the current expensive methods of removing dyes from wastewater using the treatment of a synthetic textile effluent containing an acide dye, Acide Orange 7 (AO7), as the adsorbate. The Amberlite FPA-98 will be, first, characterized in terms of chemical composition, structure and texture. Adsorption studies were carried out under various parameters such as average agitation, pH, mass of adsorbent, contact time, initial dye concentration and temperature. The adsorption kinetic data of the Amberlite FPA-98 was tested by pseudo-first-order, pseudo-second-order kinetic and Elovich models in order to estimate quantitatively their influence on dye removal and to determine the rate limiting step of dye adsorption. The equilibrium data were analyzed using Langmuir, Freundlich and Temkin isotherm models. Moreover, a thermodynamic study of the adsorption isotherms will be carried out and the results will be confronted to conventional models, so that the thermodynamic properties could be used to determine the mechanism of dye removal.

2. Material and Methods

Porous Polymers (Resin Adsorbent): Amberlite FPA 98

There are two main criteria for the choice of adsorbent: The maximum adsorption capacity (q_m): solute concentration transmitted in the solid phase, must be maximized. The adsorption kinetics: the adsorption must take place rapidly. Exchange resins, strongly basic anionic ion, the principle is to exchange certain ions, or all with active groups on the resins. Resins, which are in the form of beads or powder form are thus able to exchange mobile ions with ions of the same sign, contained in a solution with which they are contacted. Strongly basic anionic resins bind the strong and weak acid anions in a pH range between 1 and 12. This type of resin is regenerated with sodium hydroxide solution

and in the form of spherical grains 0.5 1.5 mm in diameter, with specific surface areas of up to 750 m^2/g. Amberlite FPA98 is unique, food-grade acrylic macroporous strong base anion resin. This use of ion exchange technology based discoloration was more effective and more economical.

The application of these adsorbents Amberlite FPA98 Cl mainly develop in water treatment in the domain refining of sugar as adsorbents dyes capturing and purification of pharmaceuticals and the guard beds for precious chromatography media.

FTIR analysis was applied to determine the surface functional groups, using FTIR spectrophotometer (SCO TECH SP-FTIR-1). The FTIR spectral analyses were recorded from 4000 to 400 cm-1 and the samples were prepared as KBr pellets under high pressure [25].

B. Adsorbate Preparation

The dye chosen in this study is the Acide Orange 7, also called Acide Orange II (Sigma-Aldrich), belonging to the family of the anionic dyes. It is representative of a textile type of pollution. Its main features are represented in Table 1; its structural formula is shown in Figure 1. Stock solutions were prepared by dissolving requisite quantity of dye without further purification in distilled water, and the concentrations used were obtained by dilution of the stock solution. The pH was adjusted to a given value by addition of HCl (1N) or NaOH (1N) [26].

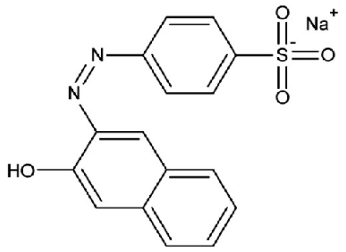

Figure 1: Molecular structure of Acide Orange 7

TABLE I : Main Characteristics of the Basic Dye Acide Orange II

Synonyme	Acide orange 7
Molecular formula	C16H11N2NaO4S
Molecular weight [g/mol]	350.33
Molecular volume (Å/molecule)	231.95
Molecular surface area (Å/molecule)	279.02
Width (Å)	7.3
Length (Å)	13.6
Depth (Å)	2.3
λ (nm)	485
pKa	pK1 11.4; pK2 1.0

C. Experimental Protocol

Adsorption Experiments and study of physico-chemical parameters

The process of the dye adsorption on the Amb.FPA98 necessarily generates a distribution of the adsorbate between the solid and liquid phases as a function of operating conditions. After study of the kinetics, isotherms and

thermodynamic parameters we're studding the influence of physico-chemical parameters such as initial dye concentration, T, pH, mass and agitation.

Adsorption Isotherms

The batch adsorption experiments were conducted in a set of 250 ml Erlenmeyer flask containing adsorbent and 200 ml of AO7 solution at various initial concentrations. The flasks were agitated in an isothermal water-bath shaker at 200 rpm and solution temperature was varied in the range (20–50°C) and all mixtures were studied until the equilibrium is reached. The filtration of the biphasic samples was carried out using disposable syringe filters with a pore size 0.45 µm that were shown first to exhibit no interaction with the dye during the sampling and to separate the solid phase from the liquid phase, the equilibrium concentrations of dye in the solution were measured at 485 nm. The pH of solutions was adjusted with 1N HCl or 1N NaOH solutions[27].

Adsorption kinetics

Adsorption kinetics were carried out to establish the influence of several parameters (contact time, temperature, initial dye concentration) using a mechanic stirrer. In the biosorption experiments, The TES was tested for the adsorption of AO7 dye from aqueous solutions at room temperature using the batch reactor technique. Adsorption kinetic experiments were performed by contacting 3L of AO7 solution at different initial concentrations ranging from 40 to 240 mg/L with 3g of Amberlite FPA98 in reactor at room temperature. At fixed time intervals, the samples were taken from the solution and were separated from the sorbent through a filter and the residual concentration was determined. Experiments were repeated for different initial AO7 concentration (40-240mg/L), agitation speed (50–250rpm) and temperature (20 - 50°C) values. PH was measured using a combination pH associated with pH-meter calibrated beforehand. The respective affects of agitation speed, pH, temperature (T), adsorbent mass (m_0) and initial dye concentration (C_0) have been investigated.

All the experiments were carried out in duplicate and mean values are presented. The dye removal percentage using Amberlite FPA98 adsorbent was calculated [28] from:

$$\mathbf{Re(\%) = 100\ x\ (C_0 - C_e)/C_0} \quad (1)$$

Where C_0 is the initial concentration of dye in solution (mg/L), and C_e is the final dye concentration in aqueous solution after phase separation (mg/L). The amount of adsorption per gram of Amberlite FPA98 at any time t, q_e (mg/g), was evaluated from the change in solution concentration using[29]:

$$q_e = (C_0 - C_e)x\frac{v}{m} \quad (2)$$

Where q_e is the uptake capacity (mg/g), C_0 and C_e (mg/L) are the liquid-phase concentrations of AO7 at initial and any time t, respectively, v is the volume of the solution (L) and m is the mass of the adsorbent (g).The analysis of the instantaneous concentration C_t in the filtered liquid phase was carried out using a double beam UV-visible absorption spectrophotometer using the wavelength of maximum absorbance of the AO7 λ_{max}=485 nm. The linearity of Beer-Lambert law was checked for concentration ranging from 1 to 50 mg/L with a correlation coefficientR^2 = 0.9997.

Isotherm Modeling

All adsorption phenomena are often addressed by their isothermal behavior. The analysis of the isotherm data is important to develop an equation which accurately represents the results and which could be used for design purposes. The isothermal curves describe the relationship at the adsorption equilibrium between adsorbed specie and an adsorbent amount in a given solvent at a constant temperature. The adsorption isotherm is important from both a theoretical and a practical point of view. The adsorption isotherms were performed with different initial concentrations in order to determine the sorption mechanisms, the surface properties and affinities of the sorbent and the adsorption saturation capacity and we have to find accurately a suitable model. By plotting solid phase concentration against liquid phase concentration graphically it is possible to depict the equilibrium adsorption isotherm [30].

In order to investigate the effect of temperature on the equilibrium capacity of Amberlite FPA98 adsorbent for the removal of AO7 from aqueous solution, the equilibrium of adsorption data was analyzed using Langmuir, Freundlich, and Temkin isotherms models. Linear regression is frequently used to determine the best-fitting isotherm, and the applicability of isotherm equations is compared by judging the correlation coefficients[31].
The theoretical Langmuir sorption isotherm is valid for adsorption of a solute from a liquid solution as monolayer adsorption on a surface containing a finite number of identical sites. The model is based on several basic assumptions [32]:
(1) Adsorption is assumed to take place at specific homogenous sites with the adsorbent;
(2) Once a dye molecule occupies a site, no further adsorption can take place at that site;
(3) The adsorbent has a finite capacity for the adsorbate (at equilibrium);
(4) All sites are identical and energetically equivalent.
Therefore, the Langmuir isotherm model was chosen for estimation of the maximum adsorption capacity corresponding to complete monolayer coverage on the sorbent surface. A mathematical expression of the generalized non-linear form of the Langmuir isotherm is given by :

$$q_e = \frac{q_{max} K_L C_e}{1+K_L C_e} \qquad (3)$$

Where C_e (mg/L) is the equilibrium dye concentration; qe (mg/g) is the adsorbed amount at equilibrium; q_{max} is the maximum adsorption capacity (mg/g); K_L is Langmuir equilibrium constant (L/mg). The linear equation of Langmuir isotherm model can be written as followed:

$$\frac{C_e}{q_e} = \frac{C_e}{q_{max}} + \frac{1}{K_L q_{max}} \quad (4)$$

The essential characteristic of the Langmuir isotherm can be expressed by the dimensionless constant called equilibrium parameter, R_L, defined by [33]:

$$R_L = \frac{1}{1+K_L C_0} \quad (5)$$

where K_L is the Langmuir constant and C_0 is the initial dye concentration. The separation factor R_L values indicate the type of isotherm to be irreversible ($R_L = 0$), favorable ($0< R_L<1$), linear ($R_L =1$) or unfavorable ($R_L>1$).
The Freundlich isotherm model is the earliest known relationship describing the sorption process. The model applies to adsorption on heterogeneous surfaces with interaction between adsorbed molecules and the application of the Freundlich equation also suggests that sorption energy exponentially decreases on completion of the sorptional centers of an adsorbent. This isotherm is an empirical equation that can be employed to describe heterogeneous systems and is expressed by the following equation [34]:

$$q_e = K_F C_e^{1/n} \quad (6)$$

Where K_f is the Freundlich constant related to the adsorption capacity. It can be defined as the adsorption or distribution coefficient and represents the quantity of dye adsorbed onto adsorbent for unit equilibrium concentration. 1/n is the heterogeneity factor is related to the adsorption intensity and n parameter is a measure of the deviation from linearity of adsorption. Its value indicates the degree of non-linearity between solution concentration and adsorption as follows: if n=1, the adsorption is linear; if the value n< 1, this implies that adsorption process is chemical; if the value n>1, adsorption is a favorable as physical process. Conversely, the values of (1/n<1) and (1/n>1) indicate a

normal Langmuir and cooperative adsorption, respectively. Equation (6) can be linearized in the logarithmic form (7) so that the Freundlich constants can be determined:

$$\ln(q_e) = \ln(k_f) + \frac{\ln(c_e)}{n} \qquad (7)$$

Temkin isotherm model contains a factor that explicitly takes into account adsorbing adsorbate/adsorbate interactions. This model suggests that because of these interactions the heat of adsorption of all the molecules in the layer decreases linearly with coverage. Adsorption is characterized by a uniform distribution of binding energies, up to some maximum binding energy. The Temkin isotherm has commonly been applied in the following form [35]:

$$q_e = \frac{RT}{b_1} \ln(k_1 C_e) \qquad (8)$$

The Temkin isotherm can be expressed in its linear form as:

$$q_e = B_1 \ln(k_1) + B_1 \ln(c_e) \qquad (9$$

$$B_1 = \frac{RT}{b_1} \qquad (10)$$

Where q_e is the adsorbed amount at equilibrium (mg/g), Ce the equilibrium concentration of the adsorbate (mg/L), k_1 and b_1 are Temkin parameters. The constant b_1 is related to the heat of adsorption. T is the absolute temperature in °K and R is the universal gas constant 8.314 (J/mol°K). The adsorption data were analyzed according to the linear form of the Temkin isotherm.

Kinetic Models

There are several kinetic equations available for analyzing experimental sorption. The studies of adsorption equilibrium are important in determining the effectiveness of adsorption; however, it is also necessary to identify the types of adsorption mechanism in a given system.

the most famous experimental models obtained in the present work was tested with Pseudo-first, Pseudo-second, intraparticle diffusion, Elovich and Bangham's models to predict the adsorption kinetic of AO7 onto Amberlite FPA98 and the kinetic data were analyzed based on the regression coefficient (R^2)and the amount of dye adsorbed per unit weight of the adsorbent.

Pseudo-First-Order Model

The adsorption kinetic data were described by the Lagergren pseudo-first-order model, which is the earliest known equation describing the adsorption rate based on the solid capacity. The Lagergren equation is generally expresses as follows:

$$\frac{dq_t}{dt} = k_1 (q_e - q_t) \qquad (16)$$

Where q_e and q_t are the adsorption capacity at equilibrium and at time t respectively (mg/g), $k_1$is the rate constant of pseudo-first order adsorption (l/min). By integration, it is found that[36]:

$$\ln(q_e - q_t) = \ln(q_e) - k_1.t \qquad (17)$$

Pseudo-Second-Order Model

The adsorption kinetic may be described by the pseudo-second order model, which is generally given as in:

$$\frac{\mathrm{d}q_t}{\mathrm{d}t} = k_2\,(q_\mathrm{e} - q_t)^2 \quad (18)$$

Where q_e and q_t are the amounts of AO7 adsorbed (mg/g) onto Amberlite FPA98 at equilibrium and at time t (min), respectively and k_2 (g/mg.min) is the corresponding rate constants of pseudo-second order adsorption. By integration, the last equation simplified and can be rearranged and linearized to obtain the following relationship[37]:

$$\frac{t}{q_t} = \frac{1}{(k_2.q_e^{\,2})} + \frac{t}{q_e} \quad (19)$$

The second-order rate constants were used to calculate the initial sorption rate, h, (mg/g.min), given by

$$h = k_2.q_e^{\,2} \quad (20)$$

Elovich Model

In reactions involving chemisorption of adsorbate on a solid surface without desorption of products, adsorption rate decreases with time due to an increased surface coverage. One of the most useful models for describing chemisorption is the Elovich model. The Elovich model equation is generally expressed as [38]:

$$\frac{\mathrm{d}q_t}{\mathrm{d}t} = \alpha \exp(-\beta\, q_t) \quad (21)$$

Where α represents the initial adsorption rate (mg/g.min) and β is the desorption constant (g/mg). After integrating for the similar boundary conditions, the following equation can be obtained as:

$$q_t = \frac{1}{\beta}\ln(\alpha\,\beta) + \frac{1}{\beta}\ln(t) \quad (22)$$

The parameters α and β can be computed from the slope and intercept of the linear plot of q_t versus ln (t).

Intraparticle diffusion Model

Adsorption is a multi-step process involving transport of the adsorbate (dye) molecules from the aqueous phase to the surface of the solid particles then followed by diffusion of the solute molecules into the pore interiors. If the experiment is a batch system with rapid stirring, there is a possibility that the transport of sorbate from solution into pores of the adsorbent is the rate-controlling step. Since the AO7 is probably transported from its aqueous solution to the Amberlite FPA98 by intraparticle diffusion, so the intraparticle diffusion is another kinetic model developed by Weber and Morris should be used to study the rate-limiting step for AO7 adsorption onto Amberlite FPA98. The intra-particle diffusion is commonly expressed by [39]:

$$q_t = k_{dif}\,(t)^{0.5} + \mathrm{c} \quad (23)$$

Where C (mg/g) is the intercept and K_{dif} (mg/gmin$^{1/2}$) is the intraparticle diffusion rate constant. The values of the amount of dye adsorbed q_t were found to give two lines part with values of the square root of time $t^{1/2}$.

Bangham's Model
It is generally expressed as[40]:

$$\log\left(\frac{c_0}{c_0 - q_t m}\right) = \log\left(\frac{k_0 m}{2.303V}\right) + \alpha \log(t) \qquad (24)$$

where C_0 is the initial concentration of the adsorbate in solution (mg/L), V the volume of the solution (l), m the weight of adsorbent used per liter of solution (g/L),q_t (mg/g) the amount of adsorbate retained at time t, $\alpha<1$ and k_0 are constants determined from the plot of $Log[C_0/C_0-mq_t]$ versus log(t).

Thermodynamic study
To investigate the adsorption processes, thermodynamic parameters such as ΔS°, ΔH° and ΔG° are calculated for the system AO7/Amberlite FPA98 at different temperatures. The evaluation of these parameters is estimated using the following relations (25-26) from the plot of ln (K_L) versus 1/T.

$$\Delta G = -RT \ln(k_L) \qquad (25)$$

$$Ln K_L = -\frac{\Delta G^\circ}{RT} = -\frac{\Delta H^\circ}{RT} + \frac{\Delta S^\circ}{R} \qquad (26)$$

Where T (°K) is the absolute temperature, R (8.314 J/ mol.K) is the universal gas constant and K_L(L/mg) is the constant of Lagmuir [41].
The activation energy of adsorption E_a must be determined;
The second order rate constant (k_2) is expressed as a function of temperature by the Arrhenius equation. The linear form between $k_2$and temperature can be applied to calculate the activation energy (E_a) of the adsorption using (28):

$$\ln(k_2) = \ln(k_0) - \frac{E_a}{RT} \qquad (28)$$

Where E_a is the activation energy of sorption (kJ/mol), k_0 is the temperature-independent factor (g/mg.min), R is the gas constant (8.314 J/mol.K) and T is the solution temperature (°K). The physisorption processes usually have activation energies in the range of 0–50 kJ/mol, while higher activation energies (50–800 kJ/mol) suggest chemisorption[42].

Studies on Point of Zero Charge (pHpzc)
In pH_{pzc} determination, 0.1M NaCl was prepared and its pH was adjusted in the range of 2–11 by adding 0.1M NaOH or HCl. Then, 50mL of 0.1M NaCl each was put in conical flask and then 0.1g of the TES was added to these solutions. These flasks were kept for 48h and final pH of the solution was measured by using pH meter. Graphs were then plotted for final pH vs initial pH [43].

3. Results and Discussion

3.1.FTIR and DRX Spectral Analysis
Analysis of FT-IR spectrum of Amberlite FPA98 adsorbent in the range of 400–4000 cm^{-1}as shown in Fig.2 shows some bands at 3450 cm^{-1}that are assigned to –OH stretching mode vibrations due to inter-and intra-molecular hydrogen bonding of polymeric compounds [44]. The peak at 2820 $cm^{-1}$is due to asymmetric stretching vibrations of C-H and the peak observed at1648 cm^{-1}can be assigned to C=O and COOH has been assigned to peaks at 1250 cm^{-1} .

The X-ray diffraction of our biosorbent is shown in Fig.3; The figure shows two main peak appeared at 2Theta =8 and 2Theta =22. In addition, this spectrum shows several other small peaks at 2Theta = 10,30 and 40 .

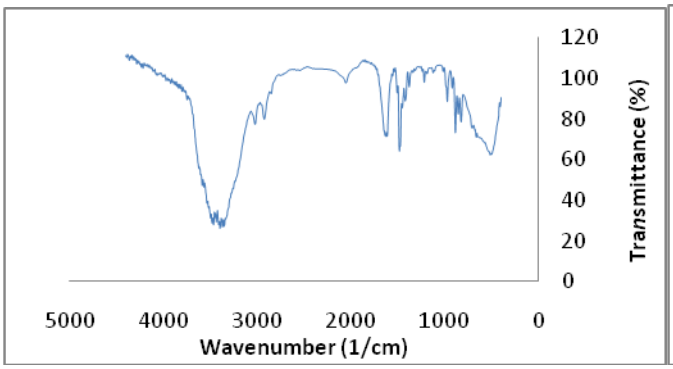

Figure 2: FTIR spectra of Amberlite FPA98

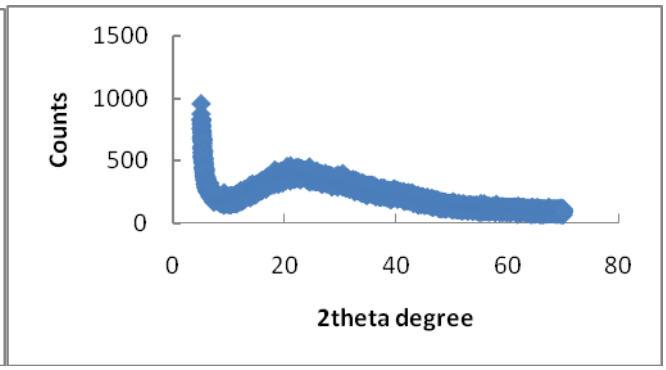

Figure 3: X-ray diffraction pattern of Amberlite FPA98

3.2. Effect of Initial AO7 Concentration and Contact Time on AO7 Adsorption

The effect of initial dye concentration, at 25°C, was carried out in the range of 40 and 240 mg/L at pH 7 with 3g of Amberlite FPA98 added in each 3 liters of AO7 solution. The experimental results showed that the adsorbed quantity increase when C_0 increases. The results obtained are shown in Fig. 4 and indicate that the uptake rate of AO7 dye adsorbed per gram of Amberlite FPA98 increase gradually as the increase in the concentration of AO7 at the beginning and, thereafter, the adsorption of AO7 reached equilibrium at 90 min. We can say that the equilibrium time is independent of the concentration and the amount adsorbed at equilibrium increases with concentration. The equilibrium adsorption increases from 80 to 180 mg/g, with increase in the initial AO7 concentration from 40 to 240 mg/L. This variation of the initial concentration generates an increase in the initial rate of adsorption. This is because the diffusion of dye molecules from the solution to the adsorbent surface is accelerated by increasing the dye concentration. The increase in uptake capacity of the sorbent with increasing AO7 concentration may be due to the increase of sorbate quantity [45].. However, the experimental data were measured at 120 min to be sure that full equilibrium was attained.

The amount of the dye adsorbed at equilibrium on Amberlite FPA98 increased with an increase in the initial dye concentration of solution to a plateau value which corresponds to the maximum capacity of adsorption. This can be explained by the fact that adsorbent had a limited number of active sites, which would have become saturated above a certain concentration.

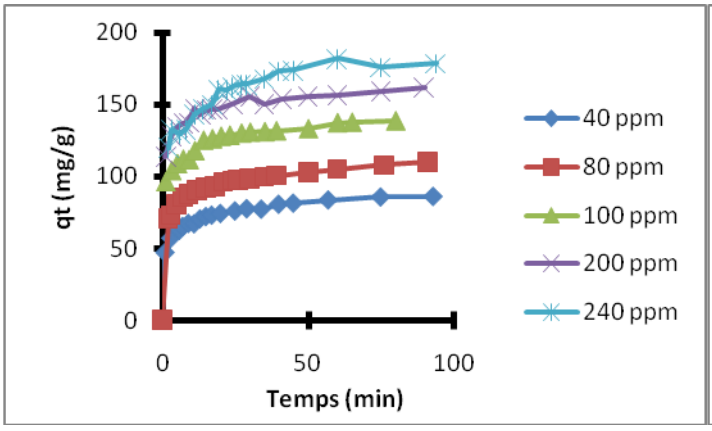

Figure 4: kinetics adsorption of AO7 by Amberlite FPA98

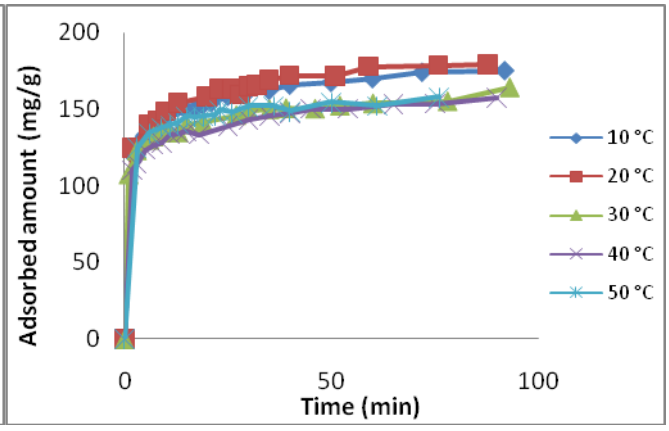

Figure 5: Effect of temperature on the adsorption of AO7

3.3. Effect of Temperature

To determine the effect of temperature on the adsorption of the AO7 dye, experiments were conducted at 10, 20, 30,40 and 50°C. The experiments were performed by adding 1 g/L of Amberlite FPA98 to the AO7 solution at a fixed concentration (80 ppm) and constant pH. The equilibrium uptake percentage of dye ions using Amberlite FPA98 was affected by temperature. So, the increase in temperature decreases the physical forces responsible for sorption. Fig.5 shows that the adsorption of AO7 by Amberlite FPA98 decreased with an increase in temperature. This behavior indicates that the AO7 dye adsorption is an exothermic process. Furthermore, the decrease uptake of the anionic AO7 dye removal at higher temperatures (above 20°C) may be attributed to the destruction of some polymeric active sites on the adsorbent surface due to bond rupture, as well as the deformation of surfaces at higher temperatures. Consequently, the study found that the dye adsorption process was affected by temperature and that the optimum working range was 20°C.

3.4. Effect of Solution pH and the Point of Zero Charge (pHpzc) on AO7 Adsorption

The pH is an important factor in the adsorption study, because it can influence at the same time the structure of adsorbent, adsorbed molecules as well as the mechanism of adsorption. This factor depends on the origin of water to be treated and the process of their treatments. The pH affects both the degree of ionization of the dye as well as the surface properties of the adsorbent. Since hydrogen ions affect the surface charge of the adsorbents and the adsorbate species, the sorption is greatly affected by the variation of solution pH. We have thus studied the efficiency of the adsorption when the pH is varied in the range of 1-12 as shown in Fig. 6. The figure indicates that, as the pH increase, the adsorption capacity for AO7 increases. Fig. 6 shows the variations of the adsorbed quantity of dye according to the initial pH of dye aqueous solutions. The figure indicates that the favorable adsorption of the dye at relatively pH ranged between 7 and 9. The adsorption capacity of the sorbent was screened over a wide pH range of the dye solution, i.e. from 1.0 to 12.0. The pH value of 7 was selected as the optimum for performing the adsorption studies. The point of zero charge (pH_{pzc}) is an important factor that determines the linear range of pH sensitivity and then indicates the type of surface active centers and the adsorption ability of the surface [46]. Cationic dye adsorption is favored at pH >pH_{pzc}, due to presence of functional groups such as OH, COO- groups. Anionic dye adsorption is favored at pH<pH_{pzc} where the surface becomes positively charged. The graph of final pH vs initial pH was plotted as shown in Fig.7.

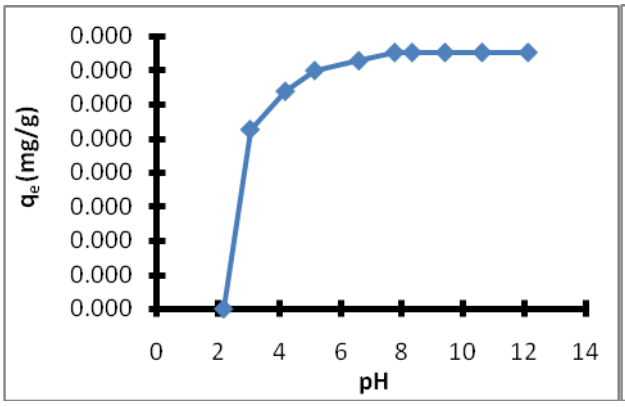

Figure 6: Effect of solution pH on the adsorption of AO7

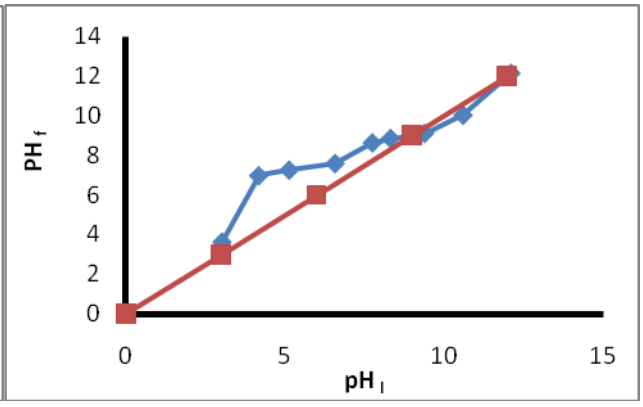

Figure 7: Determination of point of zero charge of Amberlite

The intersection of the curves with the straight linear known as the end points of the pH_{pzc}, and this value is 9 for Amberlite FPA98. As shown in Fig.6, the quantity adsorbed of dye was minimum at pH = 2, this increased up to 9 and remained nearly constant over the initial pH ranges of 9–12. This phenomenon occurred due to the presence of H^+ ions excess in the adsorbate and the negatively charged surface of the adsorbent. Lower adsorption of AO7 at acidic pH (pH <pH_{pzc}) is due to the presence of H^+ ions excess competing with the cation groups on the dye for adsorption sites. At higher solution pH (pH>pH_{pzc}), the Amberlite FPA98 possibly negatively charged and enhance

the positively charged dye cations through electrostatic forces of attraction. We selected pH=9 for adsorption and kinetic experiments.

3.5.Effect of the Mass of Adsorbent

The influence of mass was tested in the interval 0-1,4g. Adsorbent dosage is an important parameter because it determines the capacity of adsorbent for a given initial concentration of dye molecules. Data obtained from the experiments with varying adsorbent dosage are presented in Fig. 4. The adsorption removal of AO7 increased from 40 to 60 % when the adsorbent dosage was increased from 0,2 to 1 g. The effect of Amberlite FPA98 amount on the percentage of dye removal was shown in Fig.8. It can be seen that the AO7 removal increases up to a certain limit and then it remains almost constant. Optimum Amberlite FPA98 dosage was found to be 1 g; this is due to the availability of an increase in the number of possible binding sites as the dose of adsorbent increased. Consequently, 1 g was used as optimal amount for further experiments. Increase in adsorption with adsorbent dosage can be attributed to increased adsorbent surface area.

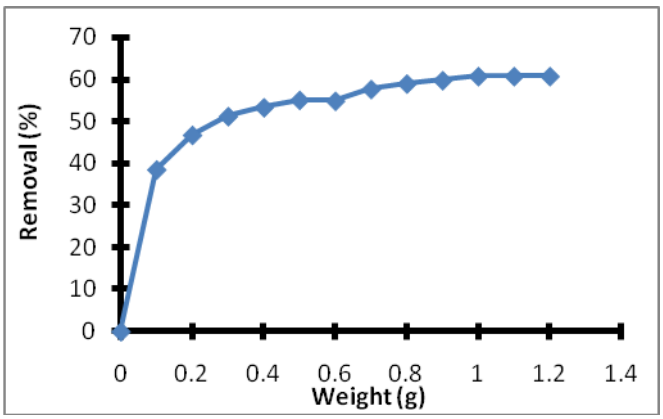

Figure 8: Effect of adsorbent dosage

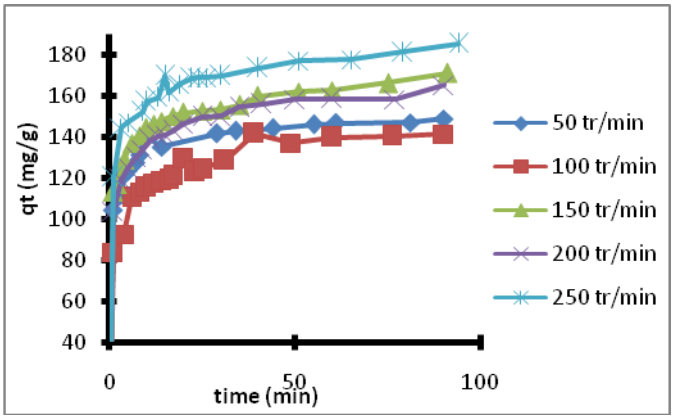

Figure 9: Effect of agitation on the adsorption of AO7 onto Amberlite

3.6. Effect of Agitation

The results of the adsorption (fig.9.) run as a function of rotation speed on the performance of adsorption, in the range studied, 50-250 rpm, show that optimal rate of agitation (200 rpm) corresponds to an adsorbed quantity associated with a maximum intra-particulate transfer coefficient. This optimal rotation speed (200 rpm) was, thus, taken as the working stirring velocity for further experiments.

3.7.Isotherm Modeling of the Sorption Equilibrium Depending on Temperature

For analyzing experimental data and for describing the equilibrium of biosorption, Langmuir, Freundlich and Temkin isotherms were simulated. Table II shows the fitting parameters for the measured isotherm data for AO7 adsorption onto Amberlite FPA98 on the linear forms of isotherms. It can be observed that the adsorption isotherm of AO7 onto Amberlite FPA98 fits Langmuir isotherm well with higher correlation coefficients (R^2) in comparison with other isotherms, reflecting that the adsorption sites on the surface of Amberlite FPA98 are evenly distributed. According to Langmuir adsorption isotherm, the q_{max} for AO7 are calculated to be 142.85, 200, 166.66, 125 and 100 $mg.g^{-1}$at 298, 303, 313, 318 and 323 °K respectively. The maximum adsorption of AO7 on Amberlite decreases with increasing the temperature, exhibiting the exothermic nature of the adsorption process. The Fig.10 shows that the top has a growth adsorbed amount qe of the dye in equilibrium when the concentration of AO7 grows, then becomes constant which reflects the saturation of the adsorption active sites. Also, the increase in temperature leads to a decrease in the adsorbed amount, it can be said that the low temperatures are of most interest and the maximum monolayer capacity q_m adsorbed at 30°C is 200 mg/g obtained from Langmuir model.

TABLE II: Comparison of the Coefficients Isotherms Parameters for AO7 Adsorption onto Amberlite FPA98

Models	T (°C) 25°C	30°C	40°C	45°C	50°C
Langmuir					
q_m(mg/g)	142.857143	200	166.666667	125	100
K_1(l/mg)	0.10144928	0.0297619	0.02521008	0.05633803	0.02369668
R^2	0.996	0.987	0.988	0.994	0.912
Freundlich					
K_f	5.98346601	6.38530975	5.40865258	4.13298539	1.46228459
N	6.4516129	6.66666667	5.58659218	3.32225914	1.55279503
R^2	0.615	0.766	0.918	0.684	0.864
Temkin					
k_1	4.67936295	7.16591949	1.93101018	0.17987572	0.02759246
B_1	20.62	21.85	21.26	36.8	43.73
b_1	8.06401552	9.51258581	11.7318909	7.90733696	6,65424194
R^2	0.594	0.755	0.899	0.6	0.85

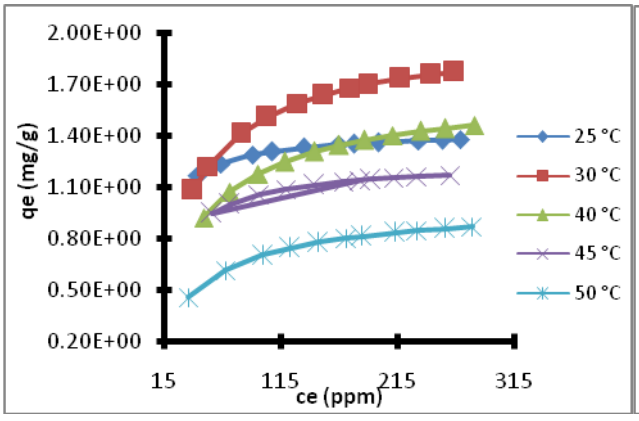

Figure 10: Variation of the adsorbed amount in terms of Ce

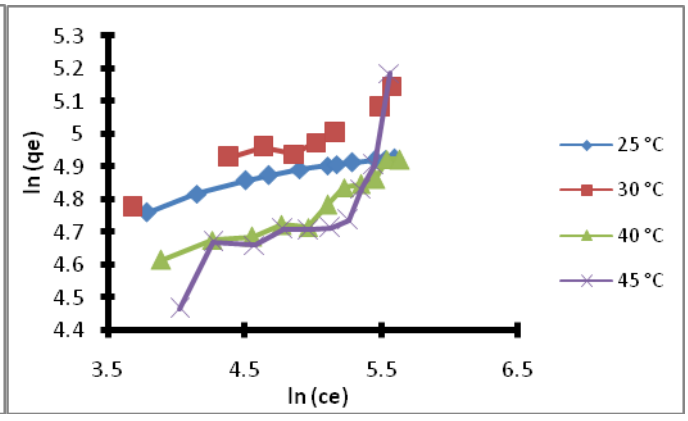

Figure 11: The plot of ln(qe) versus ln(Ce) obtained from different temperatures

The separation factor R_L values for the sorption of AO7 dye on the Amberlite FPA98 adsorbent at different initial dye concentrations have been studied at different solution temperatures**.** All R_L values fall between zero and one; This fact supports the previous observation where the Langmuir isotherm was favorable for dye sorption for all studied temperatures. Freundlich constants can be determined from the plot of ln(q_e) versus ln(C_e) (fig.11.). Thus we can generate the value of K_F from the intercept and 1/n from the slope and coefficients of determination are presented in

Table II. Freundlich model is not comparable to that obtained from Langmuir model linear form. This result indicates that the experimental data were not fitted well Freundlich model (low correlation coefficient). The values of n_f are higher than unity, indicating that adsorption of AO7 onto Amberlite FPA98 is a favorable physical process (obtained in Table II).
The Temkin constants k_1 and B_1 are calculated from the slope and the intercept of q_e versus lnC_e. The linear isotherm constants and coefficients of determination are presented in Table II. Examination of the data shows that the Temkin isotherm is not applicable to the AO7 adsorption onto Amberlite FPA98 judged by low correlation coefficient (R^2).

3.8. Thermodynamic Parameters of Adsorption
Thermodynamics experiments were carried out at a temperature range of 25-50°C. Fig.13 shows the plot of ln K_l versus 1/T and the values of estimated thermodynamic parameters are given in Table III.

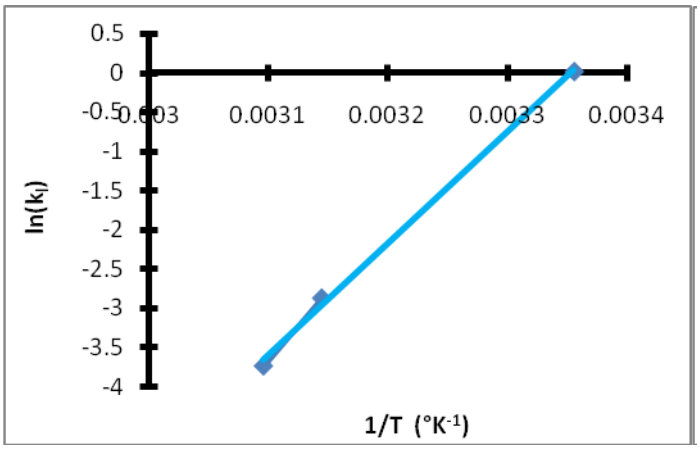

Figure 13: Plot of the adsorption of AO7 species onto Amberlite

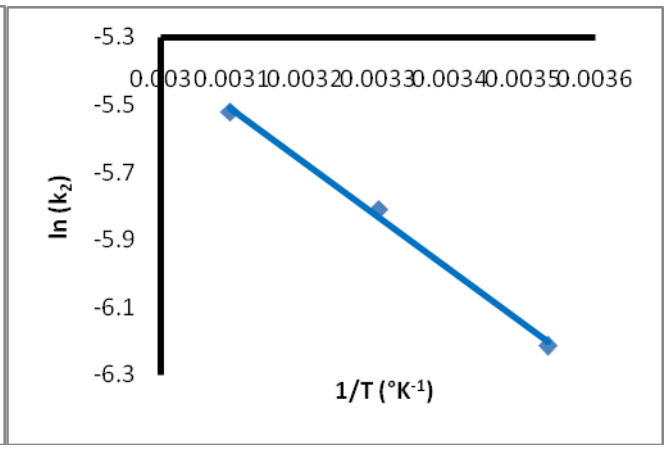

Figure 14: Arrhenius plots for the adsorption of AO7 onto Amberlite .

As can be observed, the negative value of ΔH° (-118.341 kJ/mol) shows that the adsorption is exothermic as process. The negative value of ΔS° (-396,8272 J/mol.°K) can be used to describe the randomness at the solid/solution interface during the adsorption process. The Gibbs energy(ΔG°) increased from -0,08696 kJ/mol to 9,83371606 kJ/mol with an increase in temperature from 298 to 323 °K indicate a decrease in feasibility of adsorption at higher temperatures and the spontaneous nature of the adsorption.

TABLE III: Thermodynamic Parameters Obtained from Isotherm Adsorption of AO7 onto Amb.

T (°C)	K_L(L/mg)	T (°K)	10^3/T(°K^{-1})	Ln(K)	ΔG (KJ/mol)	ΔH (J/mol)	ΔS (J/mol*°K)
25	1.01449275	298	3.3557	0.0143887	-0.08696444		
30	2.98E-02	303	3.30033		1.89717166		
40	2.52E-02	313	3.19489		5.86544386	-118341.476	-396.8272
45	5.63E-02	318	3.14465	-2.876386	7.84957996		
50	2.37E-02	323	3.09598	-3.74242	9.83371606		

Concerning the evaluation of the activation energy (E_a) of the adsorption, the Fig. 14 shows a linear relationship between the logarithm of rate constant and the inverse temperature and gives an estimation value E_a =-13.194 kJ/mol and k_0=0.55266679 (g/mg.min). The negative values of E_a indicate the presence of an energy barrier in the adsorption and confirming the nature of physisorption processes of AO7 on the surface of Amberlite FPA 98.

Kinetic Models

The most famous experimental models obtained in the present work was tested with Pseudo-first, Pseudo-second, intraparticle diffusion, Elovich and Bangham models to predict the adsorption kinetic of AO7 on Amberlite FPA98.

The adsorption data were analyzed according to the pseudo first-order kinetic model at various effects (agitation. concentration and temperature). The plots of ln ($q_e - q_t$) versus t obtained are presented in Fig.15. We can see that the first order kinetic model is not checked for all effects because the curves are not perfectly linear with lower values of R^2. It is therefore imperative to check the second order model.

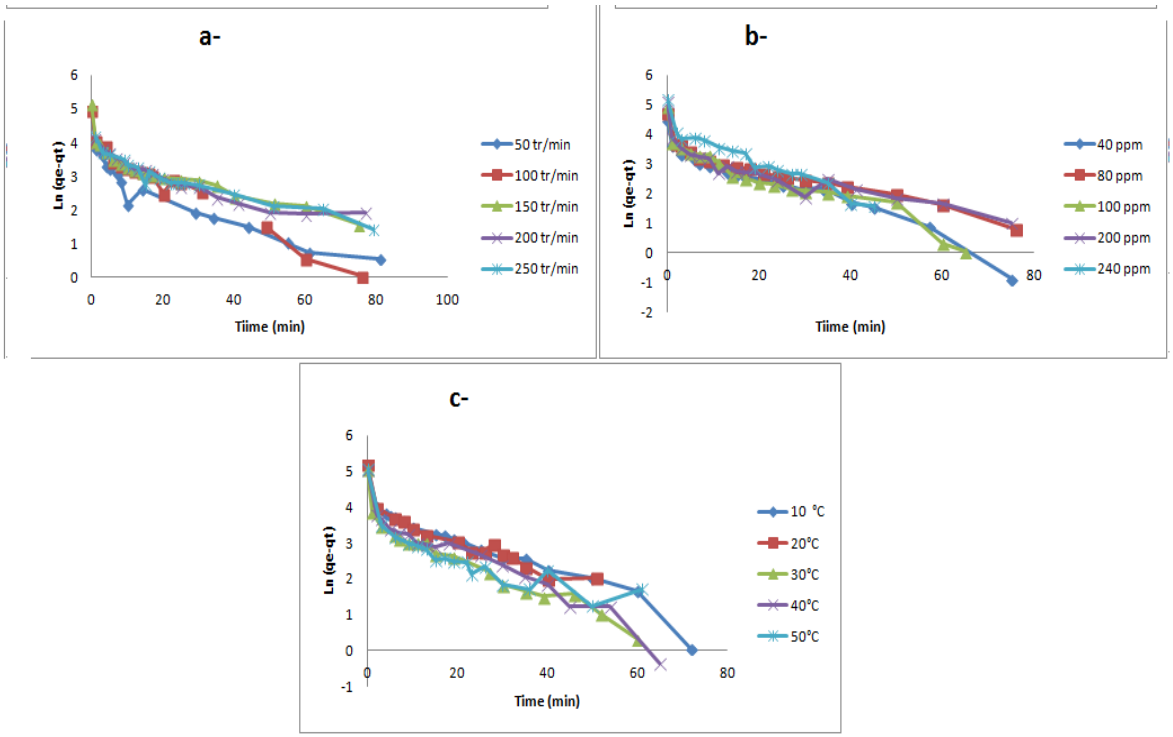

Figure 15: Pseudo-first-order kinetics for AO7 adsorption onto Amberlite FPA98 at various effects (a-agitation, b-concentration and c-temperature)

Fig.16 shows the applicability of the pseudo-second-order equation for all effects (agitation, concentration and temperature), with a coefficient of correlation R^2 greater than 0.99.Values of the rate constant k_2 and equilibrium adsorption capacity q_e were calculated from the intercept and slope of the plots of t/q_t versus t respectively.

In the table IV presents all of the results concerning the characteristics of the pseudo-first-order model and the pseudo-second-order kinetic models. This indicates that the AO7- Amberlite adsorption system obeys the pseudo-second-order kinetic model for the entire sorption period. The value of initial sorption h (mg/g.min) decreases practically with the increasing of temperature from 10 to 50°C. It was observed that the pseudo-second-order rate constant (k_2) increased with increasing of temperature from 10 to 50°C respectively. However, the results obtained using the pseudo-second-order model are not enough to predict the diffusion mechanism.

The Elovich parameters α and β and Bangham's model constant can be computed from the slope and intercept of the linear plots of q_t versus Ln (t), and Log[$C_0/C_0 - mq_t$] versus log(t) respectively at various effects (agitation. concentration and temperature) as shown in Fig. 17 and Fig.18.

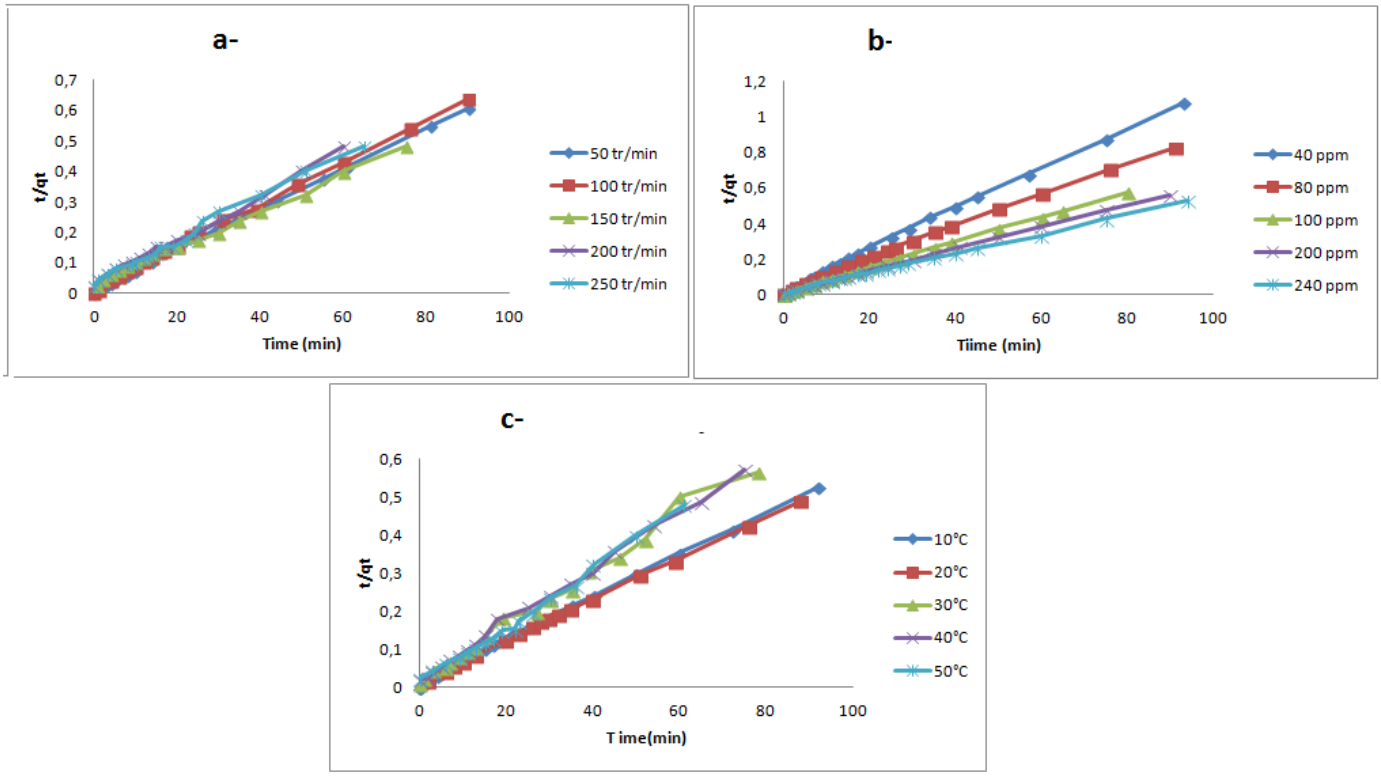

Figure 16: Plot of the pseudo-second-order model at various effects (a-agitation, b- concentration and c-temperature) of AO7 onto Amberlite

TABLE IV **:** Comparison of the First- and Second-Order Adsorption Rate Constants and qe Values for various effects (agitation, concentration and temperature) AO7 onto Amberlite

Effect	agitation	C reel	T(°C)	Pseudo 1st order			Pseudo second order			
				k_1 (l/min)	qe (mg/g)	R_1^2	$10^{-3}.k_2$ (g/mg min)	qe (mg/g)	h (mg/g.min)	R_2^2
agitation (tr/min)	50	119.67	30	0.041	32.75	0.852	6	166.66	166.66	0.999
	100	83.73	30	0.054	56.26	0.934	2	166.66	166.66	0.998
	150	111.30	30	0.033	49.30	0.805	0,6	200	26.31	0.993
	200	107.11	30	0.03	40.16	0.883	1,4	142.857	28.57	0.994
	250	109.44	30	0.029	38.82	0.898	1,48	142.857	30.30	0.992
Temperature (°C)	200	108.51	10	0.047	61.68	0.93	2	200	83.33	0.998
	200	108.04	20	0.05	65.10	0.83	2	200	83.33	0.998
	200	111.65	30	0.057	44.92	0.895	3	166.66	90.90	0.997
	200	110.95	40	0.054	50.04	0.874	3	166.66	83.33	0.998
	200	118.16	50	0.042	33.85	0.669	4	166.66	125	0.999
Concentration(ppm)	200	40	30	0.054	38.86	0.932	4	90.90	33.33	0.998
	200	80	30	0.037	39.05	0.88	3	111.11	45.45	0.998
	200	100	30	0.055	44.74	0.895	4,4	142.85	90.90	0.999
	200	200	30	0.037	37.07	0.765	4,5	166.66	125	0.999
	200	240	30	0.064	79.83	0.92	1,9	200	76.92	0.998

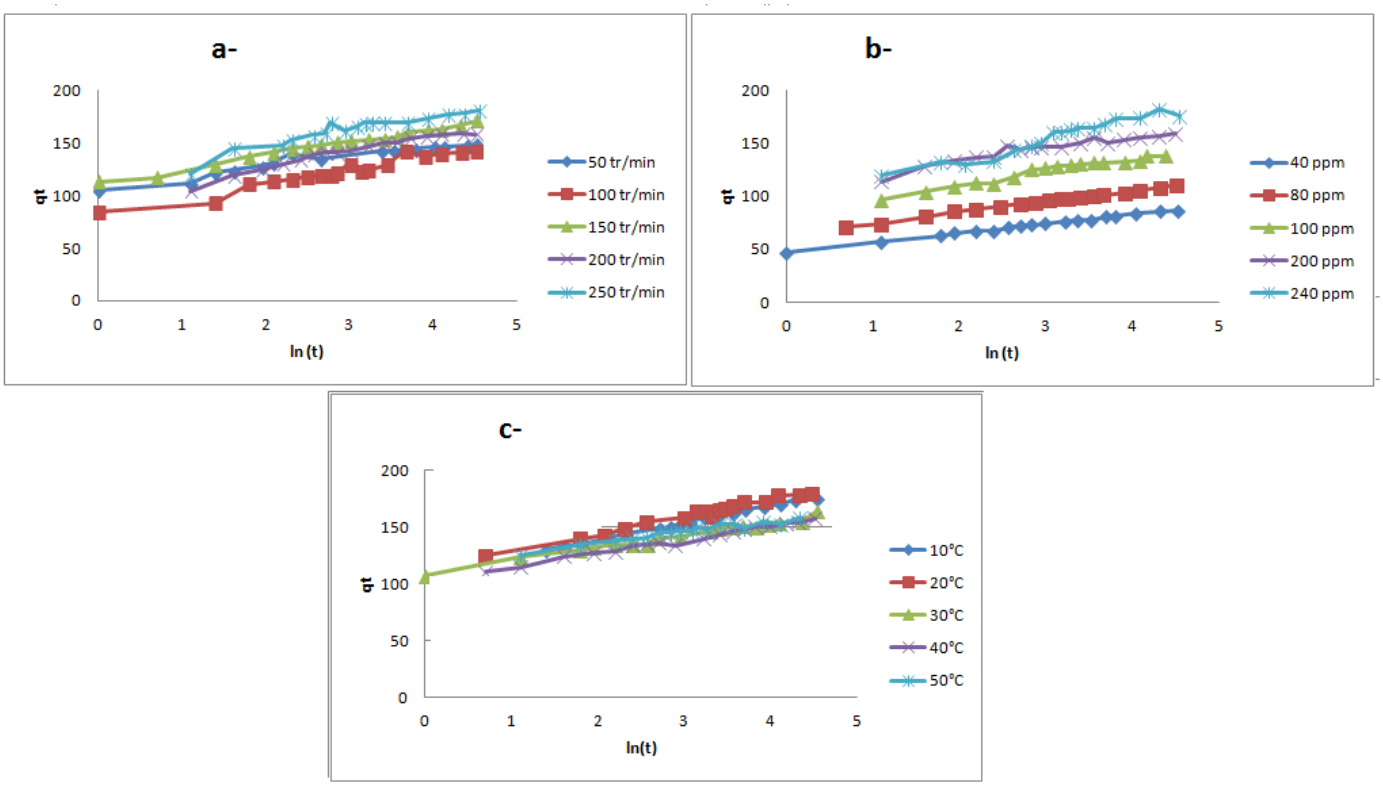

Figure 17: Elovich model plot for the adsorption of AO7 onto Amberlite FPA98 at various effects (a-agitation, b-concentration and c-temperature)

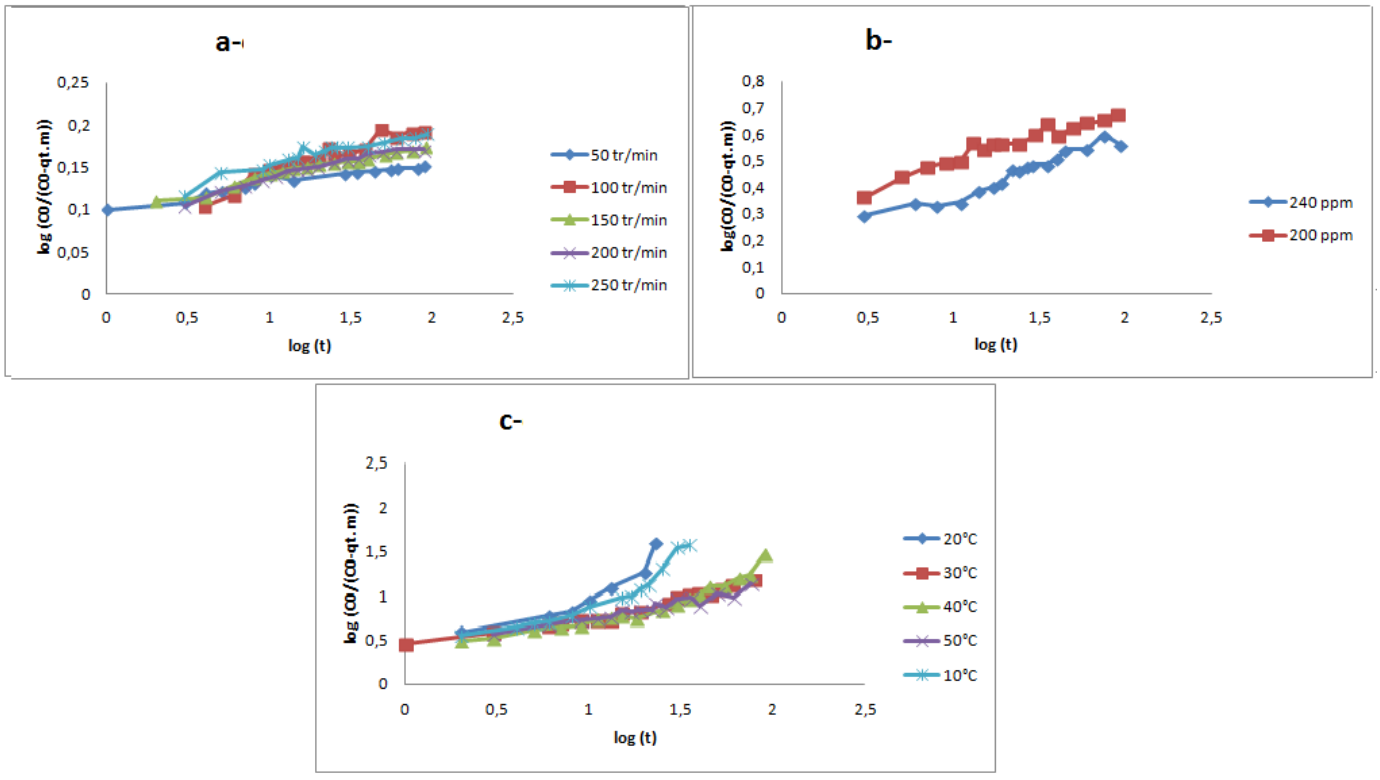

Figure 18: Bangham model plot for the adsorption of AO7 onto Amberlite FPA98 at various effects (a-agitation , b-concentration and c-temperature)

The Table V lists the kinetic constants α and k_0 obtained from the Bangham's equation. Thus, when temperature passed from 10 to 50 ◦C, the value of α decreased from 0.816 to 0.365 and the value of k_0 decreased from 5109.93 to 2886.79(mL/g/L). The experimental data did not give a good correlation. In addition, it was found that the correlation coefficients for the Elovich model are higher than those obtained for Bangham's model (Table V). This result confirmed that the pore diffusion is not the only rate-controlling step.

TABLE V : Comparison of Elovich and Bagham models parameters for various effects (agitation. concentration and temperature)

Effect	agitation	Creel	T(°C)	Elovich			Bangham		
				□ (g/mg)	α (mg/g min)	R^2	k_0(mL/g/L)	α	R^2
T(°C)	200	108.510998	10	0.06640106	20.534	0.995	5.109	0.816	0.868
	200	108.045685	20	0.06591958	26.582	0.983	4.471	0.854	0.829
	200	111.651861	30	0.0890472	18.602	0.982	2.974	0.402	0.952
	200	110.953892	40	0.08244023	55.788	0.988	4.260	0.525	0.898
	200	118.166244	50	0.10598834	23.414	0.946	2.886	0.365	0.931
C(ppm)	200	40	30	0.11313497	18.915	0.995			
	200	80	30	0.09823183	55.41	0.992			
	200	100	30	0.09416196	71.687	0.967			
	200	200	30	0.09910803	10.960	0.964			
	200	240	30	0.05813953	78.85	0.939			
agitation	50	119.678511	30	0.10307153	64.250	0.927	5.450	0.025	0.932
	100	83.7330795	30	0.07199424	51.65	0.945	5.500	0.05	0.944
	150	111.302876	30	0.0792393	94.620	0.985	5.387	0.034	0.986
	200	107.115059	30	0.06447453	69.73	0.954	5.450	0.038	0.989
	250	109.441624	30	0.06671114	35.807	0.887	5.228	0.036	0.969

The intraparticle diffusion is another kinetic model developed by Weber and Morris that should be used to study the rate-limiting step for AO7 adsorption onto Amberlite. The intraparticle diffusion is the sole rate-limiting step only if the plots of q_t versus $t^{1/2}$ pass through the origin, which is not the case in Fig.1**Erreur ! Signet non défini.**9.
The intraparticle diffusion rate constant K_{dif} were in the range of 0.358 –1.181 mg/g.$min^{1/2}$ and it increases with an increase of temperature. For intraparticle diffusion plots, the first sharper region is the instantaneous adsorption or external surface adsorption that can be attributed to the film diffusion.
The second region is the gradual adsorption stage where intraparticle diffusion is the rate limiting. It confirms that intraparticle diffusion was not the only rate limiting mechanism in the sorption process.
The values of $k_{diff1}$and k_{diff2} as obtained from the slopes of the two straight lines are listed in Table VI. The values of the intraparticle diffusion rates k_{diff1} are smaller than the film diffusion rates k_{diff2} .That gives prediction that the dye sorption process may be controlled by the intraparticle diffusion.

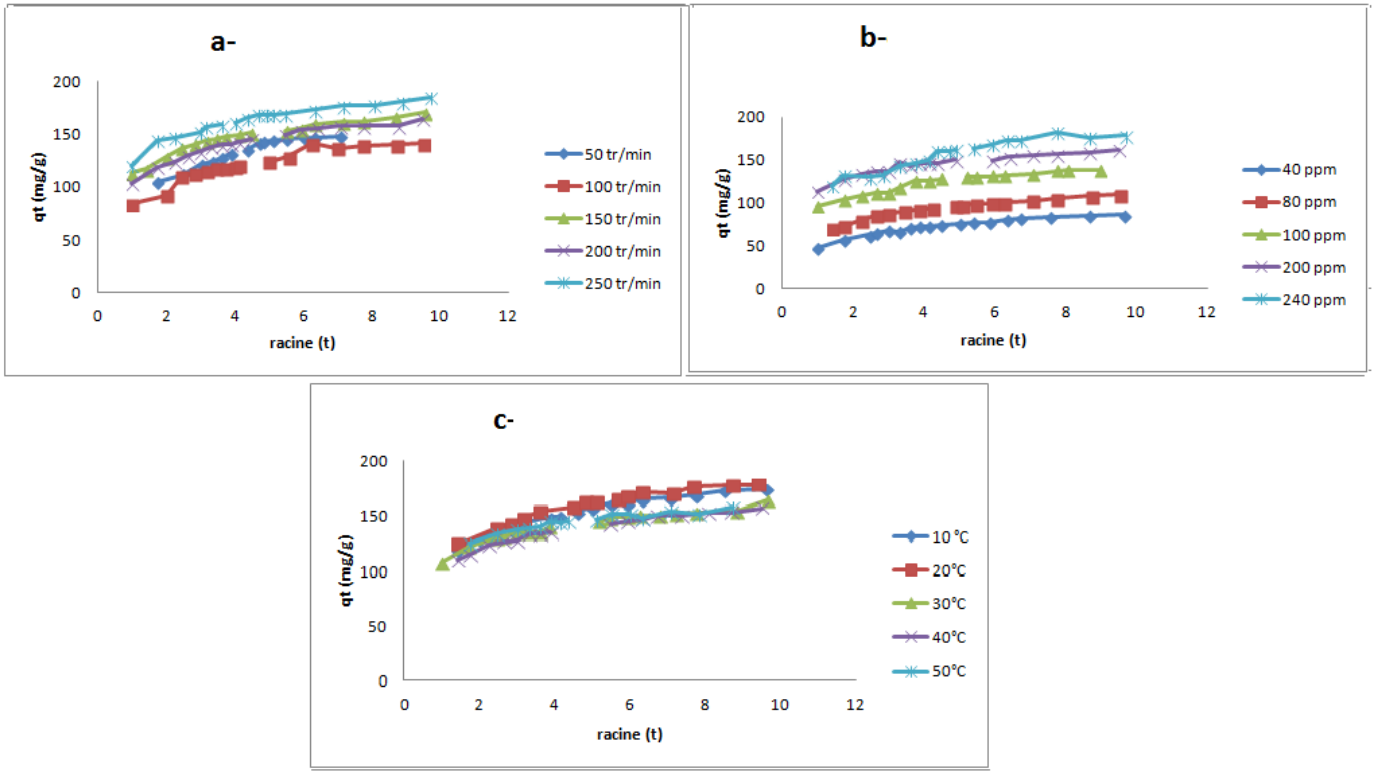

Figure 19: Intraparticle diffusion model plot for the adsorption of AO7 onto Amberlite FPA98 at various effects (a-agitation , b-concentration and c-temperature)

TABLE VI: Parameters Obtained from Intraparticle Diffusion Model for various effects (agitation. concentration and temperature)

Effect	agitation	Creel	T(°C)	intraparticle diffusion		R^2	Extraparticle diffusion		R^2
				Kdif	C		Kdif	C	
T(°C)	200	108.510998	10	10.95	107.2	0.971	4.312	136.3	0.951
	200	108.045685	20	10.37	113.1	0.967	3.475	148.1	0.873
	200	111.651861	30	10.03	102.7	0.896	3.191	130.1	0.869
	200	110.953892	40	10.36	97.63	0.96	3.283	126.4	0.956
	200	118.166244	50	7.746	113.6	0.953	2.176	137.7	0.648
C(ppm)	200	40	30	8.526	40.8	0.953	2.596	62.95	0.958
	200	80	30	8.327	60.66	0.942	2.866	82.93	0.999
	200	100	30	9.405	87.04	0.973	2.577	116.3	0.948
	200	200	30	8.64	111.7	0.889	3.007	133.3	0.964
	200	240	30	11.65	104.6	0.934	3.117	151.1	0.626
Agitation (tr/min)	50	119.678511	30	12.64	82.07	0.991	3.966	122.2	0.745
	100	83.7330795	30	12.09	74.21	0.9	3.279	112.7	0.608
	150	111.302876	30	11.53	104.5	0.944	4.007	132.2	0.96
	200	107.115059	30	11.58	97.11	0.959	2.788	136.8	0.82
	250	109.441624	30	13.36	113.8	0.873	3.565	150.1	0.965

The plot of constant of Weber and Morris equation depending on the concentration (Fig.20) shows that the diffusion constant(C) increases with increasing of the concentration in a linear fashion. This confirms that the limitante step is the intra-granular distribution.

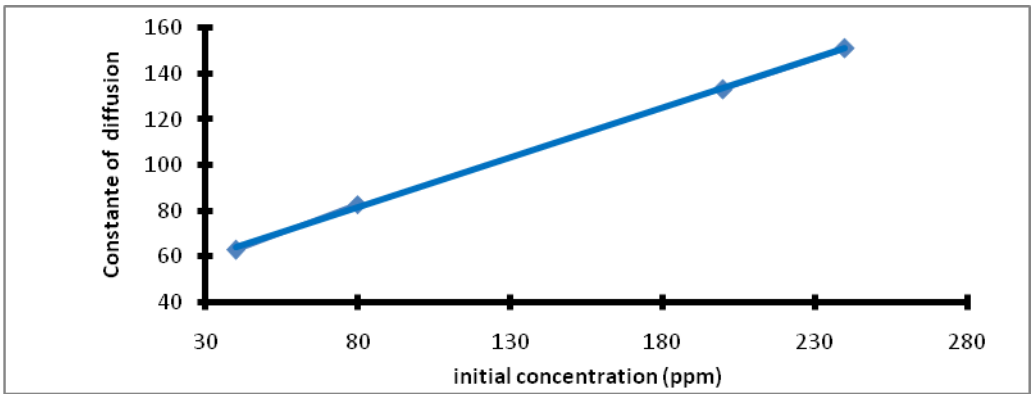

Figure 20: The variation of the constant of Weber and Morris equation depending on the concentration.

Conclusion

The efficiency of Amberlite FPA98 in removing the anionic dye AO7 dye from aqueous solution has been investigated. Amberlite FPA98 could almost remove over 75% of AO7 within 100 min contact time; the solution pH has important bearing on the extent of this process. This indicates that the pH is more important in the controlling of adsorption rather than the nature of the surface sites. This work confirms that the Amberlite FPA98 could be used for the removal of dyes from aqueous solutions.

The equilibrium time is independent of the concentration and the amount adsorbed at equilibrium increases with concentration. This is because the diffusion of dye molecules from the solution to the surface of the adsorbent is accelerated by increasing the dye concentration. The adsorbed amount decreases with increasing temperature. Results indicate that the adsorption isotherm data were fitted good agreement with the Langmuir isotherm model by comparing the values of the linear correlation coefficient R^2. The adsorption capacity was found to be 200mg.g^{-1}at 293°K. The adsorption process followed pseudo-second order kinetics and was spontaneous and exothermic. This study shows that Amberlite FPA98 is an effective adsorbent for removal of organic pollutants from aqueous solutions.

References

1. Iqbal M.J., Ashiq M.N., *J. Hazard. Mater.*139 (2007) 57–66.
2. Santos A.B., Cervantes F.J., Lier J.B., *Biores. Technol*.98 (2007) 2369–2385.
3. Vandevivere P.C., Bianchi R., Verstraete W., *J. Chem. Technol. Biotechnol.* 72 (1998) 289–302.
4. Qureshi K., Ahmad M.Z., Bhatti I.A., Iqbal M., Khan A., *Chemistry International* 1 (2015) 53-59.
5. Barka N., Assabbane A., Nounah A., Ait-Ichou Y., *J Hazard Mater* 152 (2008) 1054–1059.
6. Itoh K., Kitade Y., Yatote C., *Bull Environ Contam. Toxicol.* 56 (1996) 413–418.
7. Pinherio H.M., Touraud E., Tomas O., *Dyes Pigments* 61(2004) 121–139.
8. Liou Y.B., Tsay R.-Y., *J. Tai. Inst. Chem. Eng.* 45 (2014) 533-540.
9. Zollinger H., *Dyes and Pigments* 12 (2003) 52-68.
10. Szyguła H., Guibal E., Ruiz M., Sastre A.M., *Colloids Surf.* 330 (2008) 219–226.
11. Özcan F., Oturan M.A., Oturan N., Şahin Y., *J. Hazard. Mater*. 163 (2009) 1213–1220.
12. Elizalde-González M.P., Hernández-Montoya V., *J. Hazard. Mater*. 168 (2009) 515–522.
13. Hunger K., *Industrial Dyes Chemistry* 26 (2003) 18-26.
14. Gupta V.K., Mittal A., Gajbe V., Mittal J., *Ind. Eng. Chem.* Res. 45 (2006) 1446–1453.
15. Hsiu M., Ting-Chien C., San-De P., Hung-Lung C., *J. Hazard. Mater.* 161 (2009) 1384–1390.
16. El Haddad M., Slimani R., Mamouni R. , ElAntri S., Lazar S. *J. Assoc. Arab Univ. Bas. Appl. Sc.*14 (2013) 51–59.
17. Wang Z., Xiang B., Cheng R., Li Y., *J. Hazard. Mater*. 183 (2010) 224–232.
18. Cheng R., Ou S., Xiang B., Li Y., Liao X., *Dyes Pigments* 26 (2010) 752–758.
19. Abramian L., El-Rassy H., *Chem. Eng. J*. 150 (2009) 403–410.
20. Bourikas K., Stylidi M., Kondarides D.I., Verykios X.E., *Colloids Surf.* 20 (2005) 9222–9230.
21. Jin X., Jiang M.q., Shan X.q., Pei Z.g., Chen Z., J. *Colloid Interface Sci.* 328 (2008) 243–247.
22. Smaranda D., Bulgariu M., Gavrilescu R., *EEMJ* 8 (2009) 1391–1402.

23. Varlikli V., Bekiari M., Kus N., Boduroglu I., Oner P., Lianos G., Lyberatos S., Isli K., *J. Hazard. Mater.* 170 (2009) 27–34.
24. Gupta V.K., Carrott P.J.M., Ribeiro Carott M.M.L., Suhas K., *Rev. Environ. Sci. Tech.* 39 (2009) 783–842.
25. Guo J.Z., Li B., Liu L., Lv K., *Chemosphere* 111 (2014) 225–231.
26. Lim L.B.L., Priyantha N., Tennakoon D.T.B., Chieng H., Dahri M.K., Suklueng M., *Arab J. Chem*. 12 (2014) 32-42 .
27. El Boujaady A. , El Rhilassi A., Ziatni M.B., El Hamri R., Taitai A., Lacout J.L., *Desalin.* 275 (2011) 10–16.
28. Tsai W.T., Hsienb K.J., Hsu H.C., Lin C.M., Lin K.Y., Chiu C.H., *Bioresour. Technol.* 99 (2008) 1623–1629.
29. Seid L., Chouder D., Maouche N., Bakas I., Barka N., J. *Taiwan Inst. Chem. Eng*. 45 (2014) 2969–2974.
30. Slimani R., Anouzla A., Abrouki Y., Ramli Y., El Antri S., Mamouni R., Lazar S., El Haddad M., J. *Mater. Environ. Sci. 2 (1) (2011) 77-87*
31. Arami M., Limaee N.Y., Mahmoodi N.M., *Chem. Eng. J*. 139 (2008) 2–10.
32. Barka N., Assabbane A., Nounah A., Laanab L., Ichou Y.A., *Desalin.* 235 (2009) 264–275.
33. Gurses A., Hassani M., Kıransan O., Açıs l., Karaca S., *J. Water Process Eng*. 2 (2014) 10–21.
34. Zheng W., Li X., Wang F., Yang Q., Deng P., Zeng G., *J. Hazard. Mater*. 157 (2008) 490–495.
35. Gonte R., Balasubramanian K., *J. of Saudi Chem.* Soc. (2013).
36. Slimani R., El Ouahabi I., Abidi F., El Haddad M., Regti A., Laamari R., El Antri S., Lazar S., *J. Tai. Inst. Chem. Eng*. 45 (2014) 1578-1587.
37. Aarfane A., Salhi M., El Krati S., Tahiri M., Monkade E.K., Lhadi M., Bensitel L., *J. Mater. Environ. Sci.* 5 (2014) 1927-1939.
38. Khaled J., El Nemr A., El-Sikaily A., Abdelwahab O., *J. Hazard. Mater.* 165 (2009) 100–110.
39. Kose T.E., Kıvanç B., *Chem. Eng. J.* 178 (2011) 34– 39.
40. Mezitia F., Boukerrouib A., *Procedia Eng.* 33 (2012) 303 – 312.
41. Tan N., Li M., Lin Y.M. , Lu X.Q., Chen Z., *Desalin.* 266 (2011) 56–62.
42. Zewail T.M., Yousef N.S., *Alex. Eng. J.* 54 (2015) 83–90.
43. Suzuki T., Timofei S., Kurunczi L., Dietze U., Schuurmann G., *Chemosphere* 45 (2001) 1–9.
44. Zhou L., Jin J., Liu Z., Liang X., Shang C., *J. Hazard. Mater.* 16 (2010) 10-15.
45. Pathani H., Sharm S., Singh P., *Arab. J. Chem.* (2013) .
46. Silva J.P., Sousa S., Rodrigues J., Antunes H., Porter J.J., Gonçalves I., Dias S.F., *Sep. Purif. Technol.* 40 (2004) 309–315.

(2017) ; http://www.jmaterenvironsci.com